Journal of the European Ceramic Society **12** (1993) 165–176

O'-Sialon Ceramics Prepared by Hot Isostatic Pressing

T. Ekström,[a] P.-O. Olsson[b] & M. Holmström[a]

[a] Department of Inorganic Chemistry, University of Stockholm, S-106 91 Stockholm, Sweden
[b] National Defense Research Establishment, S-172 90 Sundbyberg, Sweden

(Received 7 August 1992; revised version received 25 February 1993; accepted 19 March 1993)

Abstract

O'-sialon ceramics, $Si_{2-x}Al_xO_{1+x}N_{2-x}$, with x = 0–0·2 have been prepared from Si_3N_4, SiO_2 and Al_2O_3 by glass-encapsulated hot isostatic pressing at 1600, 1750 and 1900°C and are compared with materials prepared by pressureless sintering at 1600 and 1775°C. Additional series were prepared with 1, 5 or 10 wt% Y_2O_3 as a sintering aid. Formation of the O'-sialon phase during sintering was dependent on the presence of a liquid phase and was promoted by alumina or yttria additions, especially when added together. Single-phase O'-sialon ceramics were never found, as small amounts of Si_3N_4 were always present. The microstructure consisted mainly of large elongated plate-like O'-sialon grains. Inclusions of β-Si_3N_4 were found in the small grains, which caused a significant amount of defects. Dense O'-sialon materials were hard (HV10 about 1500) and brittle (K_{1C} about 3·5 MPa $m^{1/2}$) at room temperature. The generally low toughness might be caused by the numerous defects in the Si_2N_2O structure in combination with a strong bond between the grains and the intergranular phase.

O'-Sialon-Keramiken, $Si_{2-x}Al_xO_{1+x}N_{2-x}$ mit x = 0–0.2, wurden aus Si_3N_4, SiO_2 und Al_2O_3 durch glasgekapseltes Heiß-Isostatisches-Pressen bei 1600, 1750 und 1900°C hergestellt und mit Material verglichen, das durch druckloses Sintern bei 1600 und 1775°C hergestellt wurde. Weiteres Material wurde mit 1, 5 oder 10 Gew.% Y_2O_3 als Sinterhilfe hergestellt. Die Bildung der O'-Sialon-Phase während des Sinterns hing von der Anwesenheit einer flüssigen Phase ab, und wurde durch Aluminiumoxid- oder Yttriumoxid-Zusätze gefördert, besonders wenn beides gleichzeitig zugegeben wurde. Einphasige O'-Sialon-Keramiken konnten nie beobachtet werden, da immer kleine Mengen von Si_3N_4 anwesend waren. Das Gefüge bestand hauptsächlich aus großen, gestreckten plattenförmigen O'-Sialon-Körnern. Einschlüsse von β-Si_3N_4, die einen erheblichen Anteil an den Defekten hatten, konnten in den kleinen Körnern nachgewiesen werden. Dichte O'-Sialon-Materialien sind bei Raumtemperatur hart (HV10 ≈ 1500) und spröde ($K_{1C} \approx 3{\cdot}5$ MPa $m^{1/2}$). Die im allgemeinen niedrige Zähigkeit wird wahrscheinlich durch die Vielzahl von Defekten in der Si_2N_2O-Struktur in Verbindung mit einer starken Bindung zwischen den Körnern und der Zwischenkornphase verursacht.

Des céramiques de type O'-Sialon—$Si_{2-x}Al_xO_{1+x}N_{2-x}$—avec x = 0 à 0·2 ont été préparées à partir de Si_3N_4, SiO_2 et Al_2O_3 par compression isostatique à chaud (1600, 1750 et 1900°C) après encapsulation sous verre. Une seconde série d'échantillons ont été préparés en ajoutant 1, 5 à 10% en poids de Y_2O_3 comme agent de frittage. Ces matériaux sont ensuite comparés à ceux obtenus par frittage naturel à 1600 et 1775°C. La formation de O'-Sialon durant le frittage dépend de la présence d'une phase liquide et est favorisée par l'addition d'alumine ou de Y_2O_3, d'autant plus lorsqu'ils sont tous les deux présents. La phase O'-Sialon coexiste toujours avec le Si_3N_4 présent à l'état de trace. La microstructure est essentiellement constituée par de gros grains O'-Sialon en forme de plaquettes alongées. Les inclusions de β-Si_3N_4 quant à elles se localisent dans les petits grains ce qui résultent en un nombre de défauts important. Des matériaux de type O'-Sialon denses se caractérisent par une grande dureté (Hv 10–1500) mais restent fragiles (K_{1C} de l'ordre de 3·5 MPa $m^{1/2}$) à température ambiante. Cette faible ténacité pourrait être causée par les nombreux défauts présents dans la structure de Si_2N_2O combinés à une forte liaison grain-phase intergranulaire.

Journal of the European Ceramic Society 0955-2219/93/$6.00

1 Introduction

The silicon oxynitride-, Si_2N_2O-, based ceramics have long been considered as promising engineering materials because of their good oxidation/corrosion resistance at high temperatures.[1-5] The refractory properties of these densely sintered materials depend on the formation of a continuous protective surface layer of silica during the early stages of oxidation. These non-oxide ceramics may have potential applications as high-temperature parts in various types of heat engines, turbines, combustion chambers, as metal cutting tools or as furnace linings in contact with molten metal or salts.

The introduction and practical use of Si_2N_2O ceramics has been slow, however, because of the difficulties in preparing fully dense bodies of single-phase materials.[6] The formation of Si_2N_2O from equimolar mixtures of high-purity Si_3N_4 and SiO_2 heated at high temperatures in the absence of sintering aids is very sluggish. It has been shown in a number of reports that additions of various sintering aids, which form a liquid phase at the sintering temperature, greatly facilitate the formation of silicon oxynitride.[7-11] The most effective sintering aids are mixtures of Y_2O_3 and Al_2O_3, which make pressureless sintering possible.[12-14] In the presence of alumina the Si_2N_2O phase forms a narrow solid solution range, called O'-sialon, represented by the formula $Si_{2-x}Al_xO_{1+x}N_{2-x}$, where x varies from 0·0 to 0·2.[13] Solidification of materials along this line, with only Al_2O_3/AlN added, gives fully dense materials by pressureless sintering at temperatures about 1800°C, but the densification process has been shown to take place at temperatures as low as 1600°C[14] with addition of Y_2O_3 and starting compositions on the Si_2N_2O–Al_2O_3–$Y_2Si_2O_7$ plane of the Y–Si–Al–O–N phase diagram.

The present study explores the effects of sintering aids, i.e. alumina and yttria additions, on the preparation and properties of Si_2N_2O ceramics by glass-encapsulated hot isostatic pressing (HIP). O'-Sialon ceramics with low alumina additions, falling within the single phase area $x = 0$–$0·2$, have been sintered with controlled amounts of yttria added. It is of special interest to minimize the yttria addition and still obtain full density materials with a high yield of the O'-sialon phase. Besides, all compositions have also been pressureless-sintered (PS) in order to obtain materials for reference, and for comparing the two sintering techniques. The results of densification, the phase analysis, the microstructure characterization and the room temperature hardness and fracture toughness measurements will be presented and discussed below.

2 Experimental

The selected compositions for this study have been made of mixtures of Si_3N_4 and SiO_2 as the parent material, with additions of Al_2O_3 corresponding to $x = 0$, 0·1 and 0·2 in the formula $Si_{2-x}Al_xO_{1+x}N_{2-x}$ and with 0, 1, 5 or 10 wt% Y_2O_3 added. The source materials used were silicon nitride (H.C. Starck-Berlin, grade LC1), silicon dioxide (Anal. purity), aluminium oxide (Alcoa, grade A16SG) and yttrium oxide (H.C. Stark-Berlin, grade Finest), see Table 1. The starting powders were carefully weighed in a total batch size of 500 g for each composition, mixed

Table 1. Characterization of the starting powders. The originally coarse-grained silica powder (surface area 0·03 m^2/g) was crushed and milled with Si_3N_4 milling balls prior to the chemical analysis and further use in the powder mixtures

Starting powder	*XRD phase contents*	*Specific surface area* (m^2/g)	*Chemical analysis* (*wt%*)					*Spectrographic analysis* (*ppm*)
			Fe	*Al*	*Ca*	*O*	*C*	
Si_3N_4	96% α-Si_3N_4 4% β-Si_3N_4	10·7	0·02	0·04	0·004	1·70	0·17	<40Ti, <20V, <40Cr, <40Mn, <40Co, <40Ni, <10Cu, <40Zn, <40As, <20Sn, <20Sb, <40Pb, <20Bi, 10Mg, <100Mo
Al_2O_3	100% α-Al_2O_3	9·2	0·005	—	0·01	—	0	80Si, <20Ti, 10V, <10Cr, <10Mn, <10Co, <10Ni, <5Cu, <20Zn, <5Sn, <10Sb, <10Pb, <5Bi, 200 Mg, <100Mo
SiO_2	100% quartz	5·7	0·05	0·05	0·01	—	0	<40Ti, <20V, <40Cr, <40Mn, <40Co, <40Ni, <10Cu, <40Zn, <40As, <20Sn, <20Sb, <40Pb, <20Bi, 400Mg, <100Mo
Y_2O_3	100% Y_2O_3	2·3	0·005	0·001	0·005	—	0·08	<40Si, <20V, <40Cr, <40Mn, <40Co, <40Ni, <10Cu, <40Zn, <40As, <20Sn, <20Sb, <40Pb, <20Bi, <10Mg

in water-free propanol and milled in a vibratory mill for 17 h with sialon milling medium. After drying, the powder mixes were dry-pressed (125 MPa) into compacts of size 16 × 16 × 6 mm. The samples were pressureless-sintered in a powder bed of submicron BN powder and in a nitrogen atmosphere at 1600 and 1775°C for 2 h, or glass encapsulated and hot isostatically pressed at 1600, 1750 and 1900°C for 2 h with 200 MPa of argon. Density measurements using Archimedes' principle were made on the as-sintered samples. The hardness (HV 10) and fracture toughness at room temperature was obtained with a Vickers diamond indenter using a 98 N (10 kg) load; the precision of repeated toughness measurements on the same sample was $\pm 0{\cdot}2\,\mathrm{MPam}^{1/2}$. The fracture toughness K_{IC} was evaluated by assuming a value of 290 GPa for Young's modulus. The phase analysis was based on X-ray powder patterns recorded with Guinier-Hägg cameras. Scanning electron microscopy (SEM) was performed on carbon-coated materials, using a Jeol JSM 6400 microscope equipped with Tracor System EDS and WDS analyzers. The crystals used for the WDS analysis were PET, TAP and for light element analysis LDEB and LDE1, making analysis down to the element Be possible. The amount of the different phases present was evaluated with the Tracor image analysis program VISTA. For transmission electron microscopy (TEM) studies, a thin circular plate was cut and dimpled to a thickness of about 40 μm, with the final thinning made by argon milling. The instruments used for TEM were a Jeol 200CX (with a top-entry, double tilt goniometer) or a Jeol 2000FX equipped with a Link EDS system.

3 Results

3.1 Densification

The HIP materials prepared at the different temperatures were examined by optical microscopy or SEM on carefully polished cross-sections and were found to be virtually pore-free, i.e. fully dense. It was found that the measured density of HIPed materials $Si_{2-x}Al_xO_{1+x}N_{2-x}$, with $x = 0$–$0{\cdot}2$, increased linearly from 2·82 to 2·94 g/cm^3 with Y_2O_3 additions increasing from 0 to 10 wt%. The small addition of alumina had no observable effect on the measured density. Since the HIP materials were pore-free their densities were assumed to be approximately equal to the densities of the PS samples.

Pressureless sintering at 1600°C of powder compacts with $x = 0$, i.e. Si_2N_2O, gave highly porous materials regardless of the level of yttria addition. PS at 1775°C, however, gave materials with a density in the range 98–99% of the densities obtained by HIP. For materials with only Al_2O_3 added, $x = 0{\cdot}1$ or 0·2, the PSed O'-sialon materials obtained at 1600°C had a higher density than the materials sintered at 1775°C. The densities of these latter materials corresponds to about 98% of the corresponding HIP materials. Addition of yttria to these O'-sialon materials gave similar results, with dense materials at the lower temperature and porosity formed at the higher temperature.

There was no measurable weight loss for the series sintered with the glass-encapsulated HIP technique. The pressureless sintered materials did however lose some weight during sintering, normally 2–5 wt% for materials with closed porosity. The highly porous materials (i.e. containing no alumina) sintered at 1600°C lost up to 15% in weight.

3.2 X-ray diffraction phase analysis

The effect of the Al_2O_3 and Y_2O_3 additions and the temperature on the formation of the O'-sialon, $Si_{2-x}Al_xO_{1+x}N_{2-x}$, phase was examined by X-ray diffraction, see summary in Table 2 and Fig. 1. Without alumina or yttria addition, only small amounts if any of the oxynitride phase were found to form from the $Si_3N_4 + SiO_2$ powder mix, regardless of preparation technique and temperature, and the samples consisted mainly of the initially added Si_3N_4 (and amorphous silica). The α-Si_3N_4/β-Si_3N_4 ratio of the starting silicon nitride powder was about 96/4 and, as seen in Table 2, some β phase formed during sintering, besides the silicon oxynitride. Occasionally a few very weak peaks occurred in the X-ray recordings, which were not possible to identify with any certainty.

Addition of alumina alone greatly favoured the O'-sialon formation, and so did an increase of the preparation temperature. These results are exemplified in Fig. 1(a) for materials either HIPed or PSed at different temperatures. At 1600°C the reaction was slow, and in the HIPed materials no O'-sialon was found. Neither did additions of yttria alone result in any formation of Si_2N_2O at 1600°C (see Table 2). With HIP technique at 1750°C, yttria addition gave an increasing amount of Si_2N_2O; a trend similar to that of increasing alumina content illustrated in Fig. 1(a). With HIP at 1900°C, however, additions of only 1 wt% Y_2O_3 greatly promoted the Si_2N_2O formation and resulted in an 87% yield. Simultaneous addition of yttria and alumina was most effective in promoting the O'-sialon formation, as demonstrated in Fig. 1(b) for $x = 0{\cdot}1$. Similar results were obtained by adding yttria to an O'-sialon of $x = 0{\cdot}2$.

Adding only alumina, aiming at compositions along $Si_{2-x}Al_xO_{1+x}N_{2-x}$, induced clearly observable shifts in the orthorhombic lattice parameters of the formed O'-sialon phase. Despite the fact that the formation of O'-sialon was about 85–95% (see

Table 2. Results of the X-ray diffraction phase analysis. An estimate of the relative amounts of α-Si_3N_4/β-Si_3N_4/Si_2N_2O after heat treatment of powder compacts. The overall compositions are represented by different x-values in $Si_{2-x}Al_xO_{1+x}N_{2-x}$ and different Y_2O_3 additions (wt%). The sintering was either pressureless sintering (PS) or hot isostatic pressing (HIP) at different temperatures for 2 h

Overall composition		*Relative amount of crystalline phases* α-Si_3N_4/β-Si_3N_4/Si_2N_2O				
$x=$	Y_2O_3	*PS1600*	*PS1775*	*HIP1600*	*HIP1750*	*HIP1900*
$x=0$	0	84/4/12	0/100/0	95/5/0	87/8/5	61/28/11
$x=0$	1	84/9/7	34/40/26	95/5/0	66/24/10	3/10/87
$x=0$	6	72/18/10	4/17/79	95/5/0	7/9/84	0/4/96
$x=0$	10	19/5/76	0/16/84	88/12/0	0/8/92	0/3/97
$x=0{\cdot}1$	0	64/19/17	3/8/89	96/4/0	6/6/88	0/10/90
$x=0{\cdot}1$	1	37/18/45	2/7/91	14/4/82	10/6/84	0/9/91
$x=0{\cdot}1$	6	8/6/86	0/10/90	8/4/88	0/7/93	0/11/89
$x=0{\cdot}1$	10	4/9/87	0/10/90	8/6/86	0/13/87	0/12/88
$x=0{\cdot}2$	0	9/3/88	2/12/86	90/10/0	0/6/94	0/5/95
$x=0{\cdot}2$	1	5/5/90	2/9/89	48/11/41	0/5/95	0/4/96

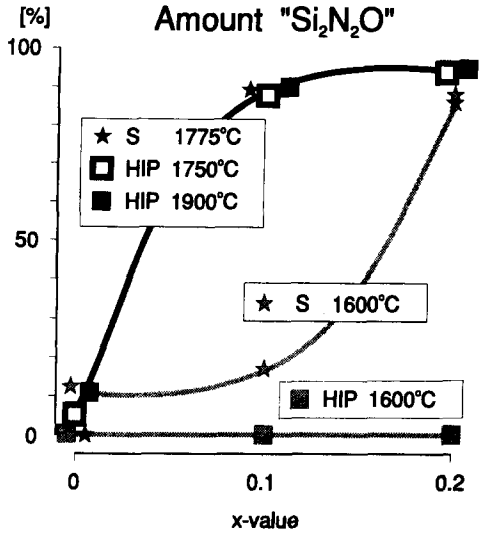

(a)

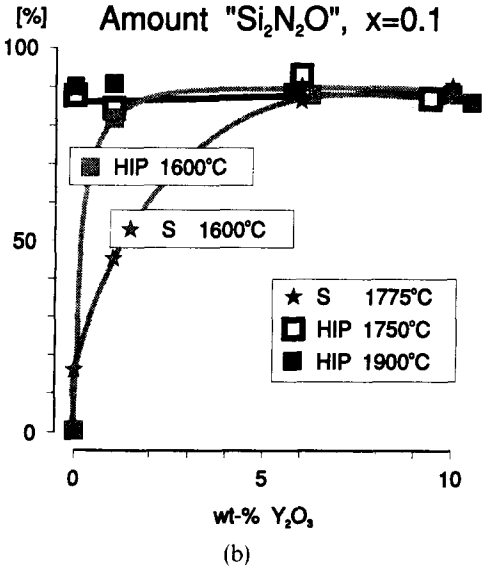

(b)

Fig. 1. The amount of Si_2N_2O or O'-sialon formed from mixtures of Si_3N_4 and SiO_2, as a function of the amount of added Al_2O_3 (the x-value), preparation temperature and method in (a). Similar presentation of the silicon oxynitride formation for a fixed value of $x=0{\cdot}1$ and varying amount of Y_2O_3 added prior to sintering in (b).

Table 2), the lattice parameters increased proportionally to the overall addition of Al (the x-value) [see Fig. 2(a)]. In materials with no alumina added, the observed orthorhombic unit cell parameters of the Si_2N_2O phase were $a=0{\cdot}8875\pm0{\cdot}0005$ nm, $b=0{\cdot}5496\pm0{\cdot}0005$ nm and $c=0{\cdot}4853\pm0{\cdot}0003$ nm. This was the case in all preparations with only yttria added and no alumina present.

Addition of yttria to O'-sialon of overall composition $x=0{\cdot}1$ or 0·2, yielded a distinct decrease in the unit cell dimensions compared with the observed parameters for the same materials with no yttria added. Thus this indicates that the O'-sialon phase loses aluminium. The observed effect of adding yttria is illustrated for an O'-sialon corresponding to an overall composition of $x=0{\cdot}1$ in Fig. 2(b). Using the lattice parameters indicated for 'pure O'-sialon' [Fig. 2(a)] as a reference, the average composition of the crystalline O'-sialon phase was found to be about $x=0{\cdot}06$ for 10 wt% Y_2O_3 added.

The cell parameters of the β-Si_3N_4 phase were observed to vary slightly as a function of starting composition and sintering temperature. For the samples with no added alumina, the hexagonal unit cell dimensions were $a=0{\cdot}760$ nm and $b=0{\cdot}291$ nm. A slight increase in cell parameters was found for the samples with alumina added. Thus $a=0{\cdot}761$ nm and $b=0{\cdot}291$ nm for $x=0{\cdot}1$ and $a=0{\cdot}761$ nm and $b=0{\cdot}292$ nm for $x=0{\cdot}2$ in samples of the overall composition $Si_{2-x}Al_xO_{1+x}N_{2-x}$. This shift indicates that a small amount of Al-O had entered the β-Si_3N_4 structure and had formed a β-sialon with a very small z-value in the β-sialon formula $Si_{6-z}Al_zO_zN_{8-z}$.[15]

3.3 Microstructure analysis by SEM

The microstructure of the materials was examined by SEM and TEM. More interest was devoted to the fully dense HIPed materials than to the porous PSed

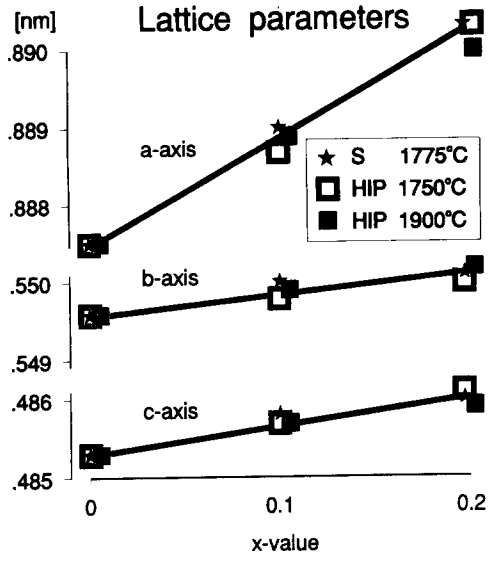

(a)

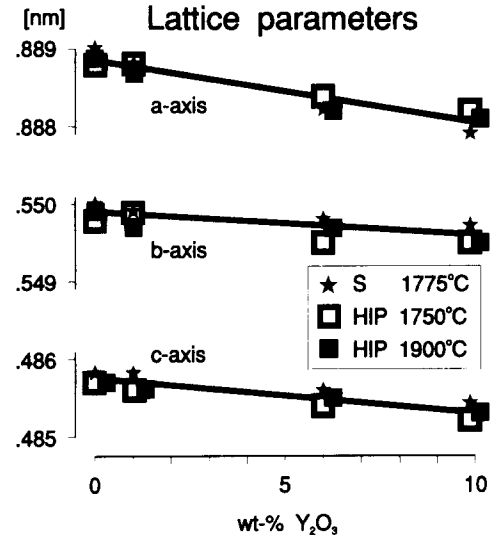

(b)

Fig. 2. Lattice parameters of the observed Si_2N_2O structure, with varying overall compositions, calculated from X-ray diffraction data and $Si_{2-x}Al_xO_{1+x}N_{2-x}$ sintered at 1750–1900°C in (a). In alumina doped specimens the O'-sialon yield was typically 85–95%, cf. Table 1. The effect on the lattice parameters of Y_2O_3 additions prior to sintering are illustrated for an O'-sialon with $x = 0{\cdot}1$ in (b).

materials. Among these samples, those sintered at 1900°C generally contained the least amount of unreacted starting materials and they were therefore considered as the most interesting in the investigated series. It can also be stated that in materials consisting of more or less unreacted starting powders the size of the grains was about 1 μm, and the microstructure showed a very poor backscatter contrast. This was especially evident for many of the samples HIPed at 1600°C. Additions of both alumina and yttria were needed to form O'-sialon in this series. An example of such a preparation, with $x = 0{\cdot}1$ and 6 wt% Y_2O_3 added, is seen in Fig. 3. The O'-sialon can be seen as long, dark crystals (about 30 vol.%) in the backscatter image, dispersed in an yttrium containing bright area, which consists of

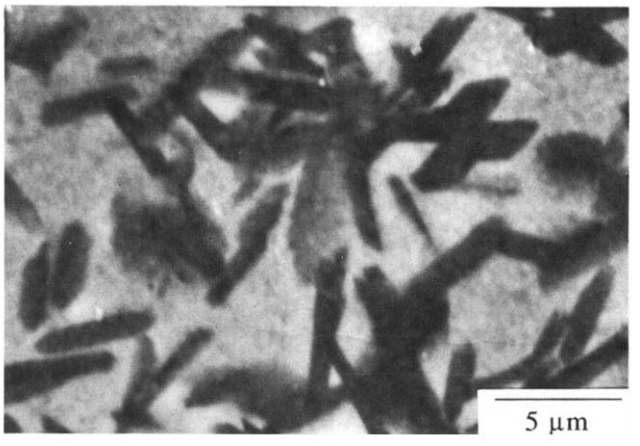

Fig. 3. Microstructure of the sample with $x = 0{\cdot}1$ and 6 wt% yttria added HIP-sintered at 1600°C, as obtained in back-scatter mode SEM.

unreacted α-Si_3N_4, according to the X-ray diffraction phase analysis, and obviously also large amounts of Y-containing glass.

A micrograph of a sample of composition $x = 0{\cdot}1$, with no yttria added HIPed at 1900°C, shows that the O'-sialon phase forms large crystals, which can be seen in Fig. 4 as elongated areas having grey contrast. The apparent cross-section of the crystals is about $2{\cdot}5 \times 12\,\mu m^2$. In addition to the O'-sialon phase which in this micrograph has grey contrast, two other contrasts can be found to a smaller extent: a black intergranular phase and bright elongated crystals with diameters below 0·5 μm. These crystals are found distributed in the amorphous intergranular phase, but some small areas of light contrast are also seen inside the large grey areas representing the O'-sialon phase.

With addition of only yttria (1 wt%) to Si_2N_2O and HIP at 1900°C, the contrast of the microstructure in SEM improved compared to that of the undoped material, so that Si_2N_2O crystals could be easily seen, as in the micrograph of Fig. 5. Only a small amount of micro-porosity or grains removed

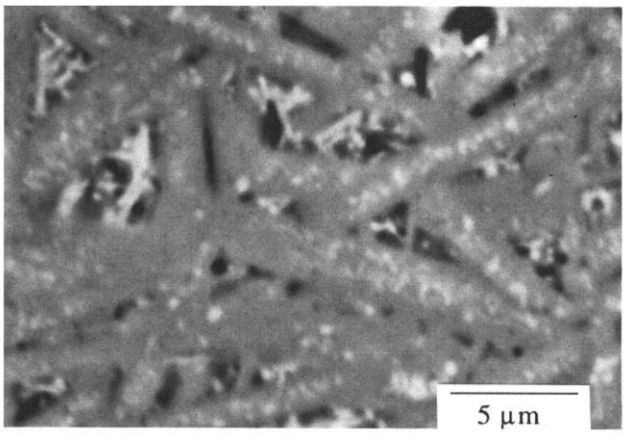

Fig. 4. Microstructure of the sample with $x = 0{\cdot}1$, no yttria added and HIP-sintered at 1900°C, as obtained in back-scatter mode SEM.

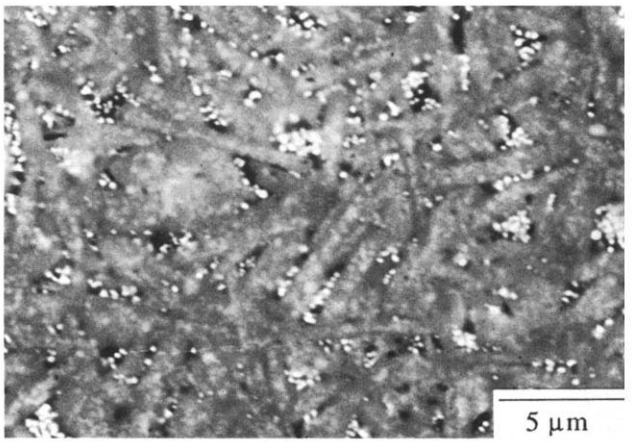

Fig. 5. Microstructure of the sample with $x=0$ and 1 wt% yttria added HIP-sintered at 1900°C, as obtained in back-scatter mode SEM.

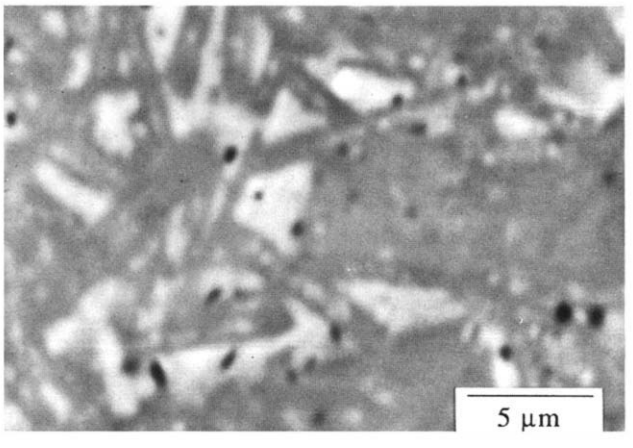

(a)

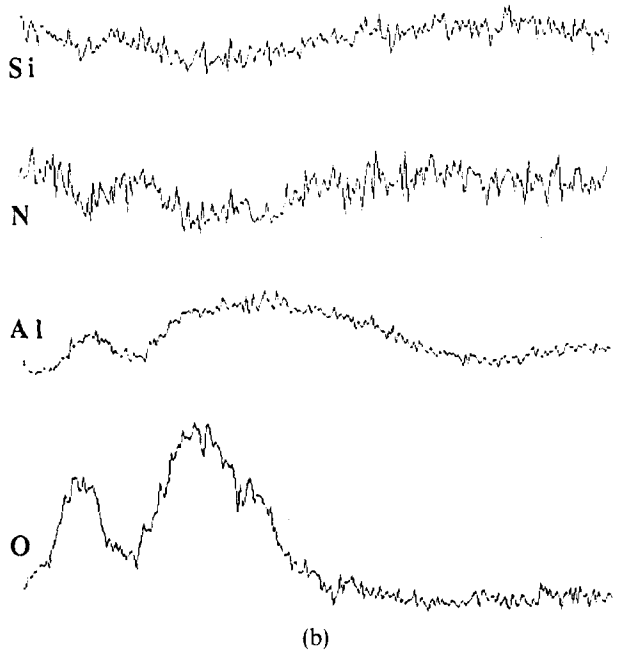

(b)

Fig. 6. Line analysis (a: white bar) of the sample with $x=0{\cdot}1$ and 1 wt% yttria added. HIP-sintered at 1900°C, showing the (b) Si, N, Al and O variation. It can be seen that the bright areas are higher in O- and Al-contrast and that the dark areas have a maximum in N and Si. Note the plate-like O′-sialon grains (see text).

in the preparation is seen as dark contrast. The Si_2N_2O-crystals have reached a diameter of about 1 μm and an aspect ratio (length to diameter) of about seven. Also, as in the case of the Al-containing material described above, small, bright areas are found at the centre of the Si_2N_2O phase region. The areas between the large crystals were found to consist of one phase giving dark contrast and one bright yttria-rich phase. The bright phase only form rounded grains, however, with a maximum diameter of about 0·5 μm. The amounts of the dark and the bright intergranular phase were about 3–4 vol.% each.

Composition analysis using the combined EDS/WDS system showed high aluminium and oxygen content in the areas having light contrast. Accordingly, the silicon and nitrogen contents were also seen to vary with the observed contrast. Thus for the dark contrast, the glassy phase had the maximum nitrogen and silicon content and was present at about 5 vol.%. Generally, the oxygen and aluminium contents were found to be conjugated, just like those of silicon and nitrogen (see the line analysis shown in Fig. 6).

Simultaneous additions of alumina ($x=0{\cdot}1$) and yttria (1 wt%) did not significantly change the appearance of the microstructure of HIPed materials compared to the samples doped with either alumina alone or yttria alone, i.e. O′-sialon were observed as elongated areas formed in an intergranular phase. Small areas of light contrast, such as described above, were also found inside the larger O′-sialon crystals, cf. Fig. 7. The addition of 1 wt% yttria gave rise to a considerable amount (about 15%) of intergranular phase in this material. Point analysis by EDS confirmed that this intergranular phase of bright contrast contained Y, Al and Si. The WDS-analysis showed the concentration of O to be higher and of N to be lower in the intergranular phase than in the O′-sialon grains.

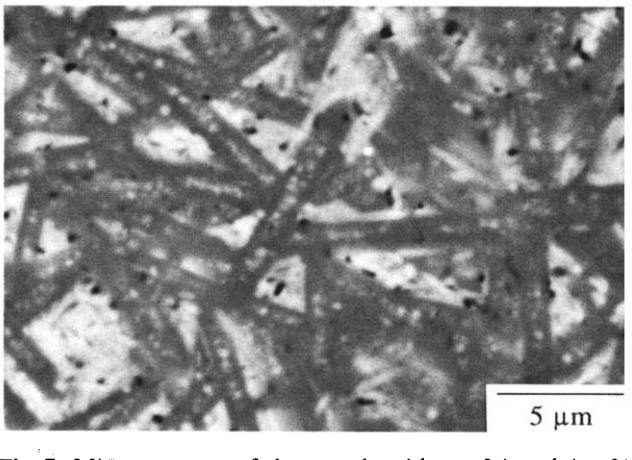

Fig. 7. Microstructure of the sample with $x=0{\cdot}1$ and 1 wt% yttria added HIP-sintered at 1900°C, as obtained in back-scatter mode SEM.

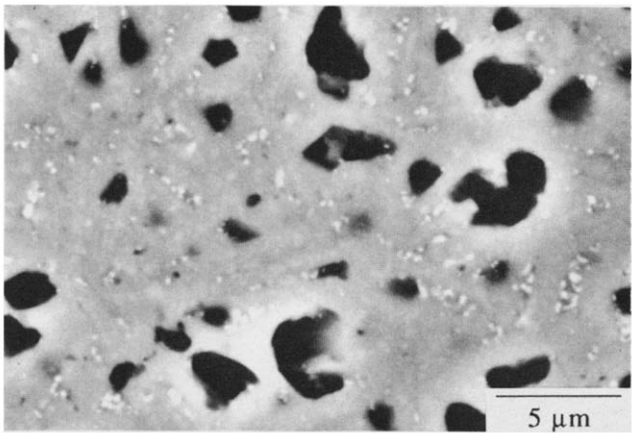

Fig. 8. Microstructures of the samples with $x = 0$ and 6 wt% yttria added pressureless sintered at 1775°C, as obtained in back-scatter mode SEM.

The PSed Si_2N_2O materials (containing no alumina) were always more or less porous, even with high Y_2O_3 additions and especially at high temperatures, as shown in Fig. 8 for additions of 6 wt% yttria and a sintering temperature of 1775°C. The pores are rounded and there is a fairly large amount of evenly distributed intergranular phase, indicating that the porosity is due to secondary gas evolution after initial consolidation. However, despite the porosity, the same type of O′-sialon grains as in the HIP-sintered samples are found, again containing small bright areas.

When comparing the different SEM microstructures (Figs 3, 4, 5, 7 and 8) the O′-sialon crystals are seen as elongated areas on the polished cross-section, giving the impression of a needle-like morphology. If, in fact, they were present in this form one would expect that some would be intersected orthogonally to the longitudinal axis of the crystal, and show a circular cross-section. Since no such structures are found it is more likely that the O′-sialon is present as elongated platelets. Indeed, on closer inspection it is possible to observe such areas having the form of a rectangle in the different microstructures, e.g. see Fig. 6.

3.4 Microstructure analysis by TEM

The HIPed sample having the initial composition of $x = 0{\cdot}1$ and 1 wt% yttria added was carefully examined by transmission electron microscopy. An example of the observed microstructure is seen in Fig. 9(a). The long, narrow crystals have been identified by electron diffraction as O′-sialon grains. In addition to these, smaller rounded crystals are found, both in the larger grains and in the intergranular regions. Finally, a glassy phase is found in the region between the O′-sialon grains.

Comparison with the SEM images shows that the large crystals correspond to the elongated crystals having dark contrast in the backscatter mode and

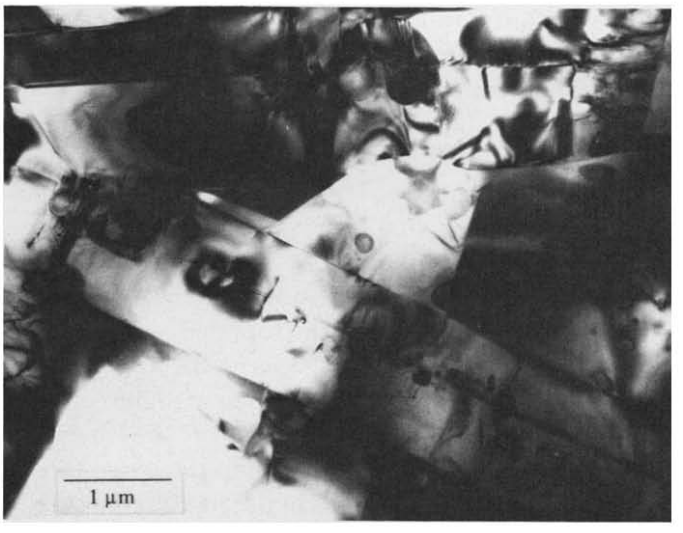

(a)

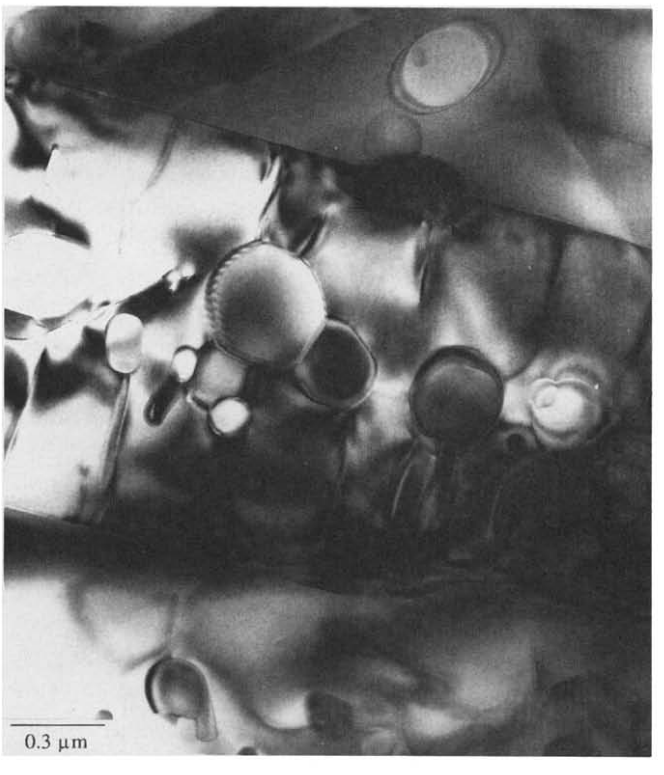

(b)

Fig. 9. TEM-images of the sample with $x = 0{\cdot}1$ and 1 wt% yttria added HIP-sintered at 1900°C at (a) low magnification and (b) high magnification. See text.

that the smaller crystals correspond to the rounded bright areas found in the SEM images. A typical Si_2N_2O crystal is shown at high magnification in Fig. 9(b). The small grains found in the O′-grain are seen to cause defects of dark contrast in the Si_2N_2O lattice (see below). One reason for this might be that the smaller grains disturb the framework of the O′-sialon crystals. However, since the grains are only seen in projection, it is difficult to rule out the possibility that some of the smaller grains are situated on the surface of the O′-sialon crystals and not inside the grains. In addition, similar types

of grains are found in the intergranular phase between the large elongated crystals.

The different types of crystals have been examined with electron diffraction. As said above, the results showed that the large elongated crystals always have the Si_2N_2O structure. However, the results of the analysis of the small crystals varied between rounded crystals found as inclusions within the Si_2N_2O grains, which when possible to identify had the β-Si_3N_4 structure, and the rounded or elongated crystals situated between the large Si_2N_2O grains. For the latter crystals, in the intergranular phase, examples of either the β-Si_3N_4 or the Si_2N_2O structure were found. In addition to these two types of structures, the occurrence of other phases in small amounts could not be ruled out, as it was not possible to identify clearly all investigated crystals.

Thus, the occurrence of rounded bright areas in the SEM analysis inside the O'-sialon grains can be explained by the inclusion of crystals having the β-Si_3N_4 structure. The fact that the β-Si_3N_4 structure contains more silicon per unit cell than Si_2N_2O (densities: Si_3N_4 3·18 and Si_2N_2O 2·82 g/cm^3) is thus enough to cause a slight difference in the back-scattered electron contrast for the two phases.

One additional feature which can be observed is the lattice defects in the oxynitride crystals. These defects are usually parallel with the elongated direction and seem to be a general feature in the O'-sialon crystals [see Fig. 9(a)]. There is also much contrast variation in the crystal images [Fig. 9(b)], which could be a result of strain in the crystals, probably caused by the defects.[16]

High resolution studies of 'Si_2N_2O' and 'β-Si_3N_4' gave no evidence for the two different crystals being structurally related. On the contrary, the two lattices showed no tendency to be aligned. This hypothesis that the structures are unrelated is strengthened by the fact that different small 'β-Si_3N_4' crystals found within the same large O'-sialon grain have no orientational relation at all. One example of such a 'β-Si_3N_4' crystal found inside a O'-sialon grain is seen in Fig. 10, where the O'-sialon is viewed along the [1 0 −1] direction with the lattice spacing of the crystal clearly visible. However, no lattice contrast appears in the 'β-Si_3N_4'-crystal. The only visible effect of the two different lattices interfering is the formation of a Moiré pattern.

X-Ray fluorescence analysis showed that neither the large O'-sialon crystals nor the small 'Si_3N_4' crystals contained any yttrium. Since the aluminium K_α-peak and the yttrium L_β-peak overlap to some extent, the K-peaks of yttrium were used for quantification of the elements. In this sample the concentration of Al varied between the different phases and different crystals. No aluminium, or very small amounts (below 0·5 at%) were observed in the O'-sialon crystals, which were thus close to pure Si_2N_2O, whereas small amounts (less than 2 at%) were detected in the silicon nitride phase. With this concentration of Al, the 'Si_3N_4' crystals can be classified as a β-sialon, $Si_{6-z}Al_zO_zN_{8-z}$, with a z-value of about 0·1.[15]

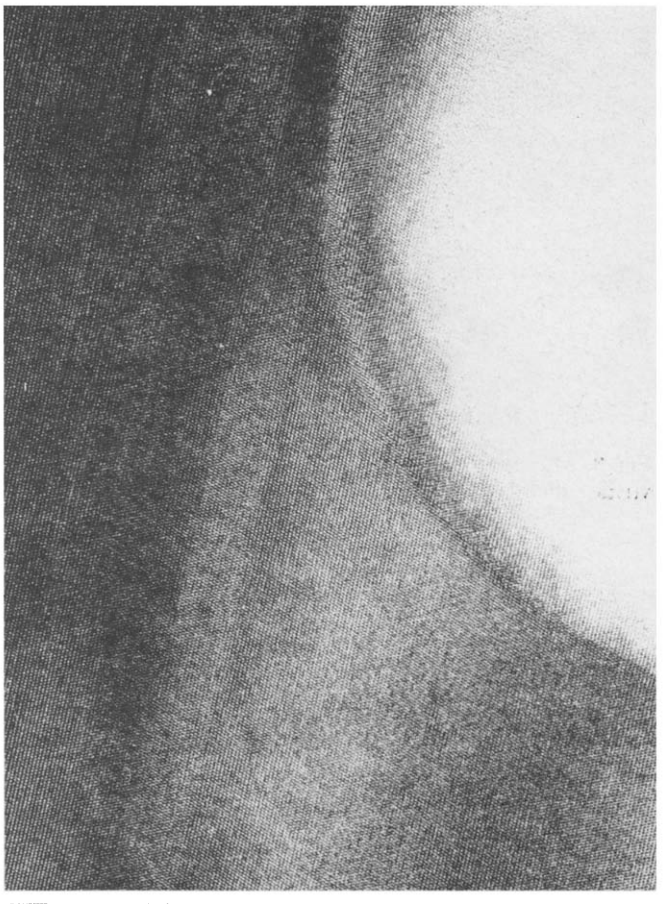

Fig. 10. A [1 0 −1] high resolution TEM-image of an Si_2N_2O crystal. The lattice spacing of the crystal is clearly seen. The diffuse white area has been identified as a β-Si_3N_4. No structural relation between the two crystal lattices was observed. The sample has $x = 0{\cdot}1$ and contains 1 wt% yttria.

Analysis of the small crystals/particles embedded in the intergranular phase showed large variation in composition. All these crystals contained large amounts of silicon, whereas the amount of aluminium varied from a few at% up to more than 20 at% Al in some of the particles. No yttrium was found in the crystalline particles. Accordingly, the amorphous structure (glassy phase) contained large amounts of yttrium. It was found that the concentration of yttrium could vary between glassy pockets from 0 at% up to about 10 at%.

3.5 Mechanical properties

The room temperature Vickers hardness (*HV10*) and indentation fracture toughness (K_{1C}) were only measured on fully dense materials prepared by HIP. No or only small amounts of Si_2N_2O were formed in the samples without sintering aid, which made it difficult to obtain the mechanical properties of a

truly monophasic Si_2N_2O ceramic material as a reference. A good approximation is, however, a Vickers hardness $HV10 = 1550$ and a fracture toughness around 3·3 MPa $m^{1/2}$ obtained on the 1900°C HIP specimen with only 1 wt% Y_2O_3 added.

Addition of only yttria (1–10 wt%) to silicon oxynitride was, independently of sintering temperature, not found to influence the fracture toughness significantly as all measured values fall in the 3–3·5 MPa $m^{1/2}$ interval. However, the hardness values showed a slightly larger dependence on the sintering temperature and amount of additions. For example, in the undoped materials the hardness increased from 1250 to about 1600 with sintering temperature (1600–1900°C). The yttria addition resulted, however, in a decrease in hardness for the Si_2N_2O series sintered at 1900°C and a slight increase in hardness for the materials sintered at lower temperature. The hardness values obtained at

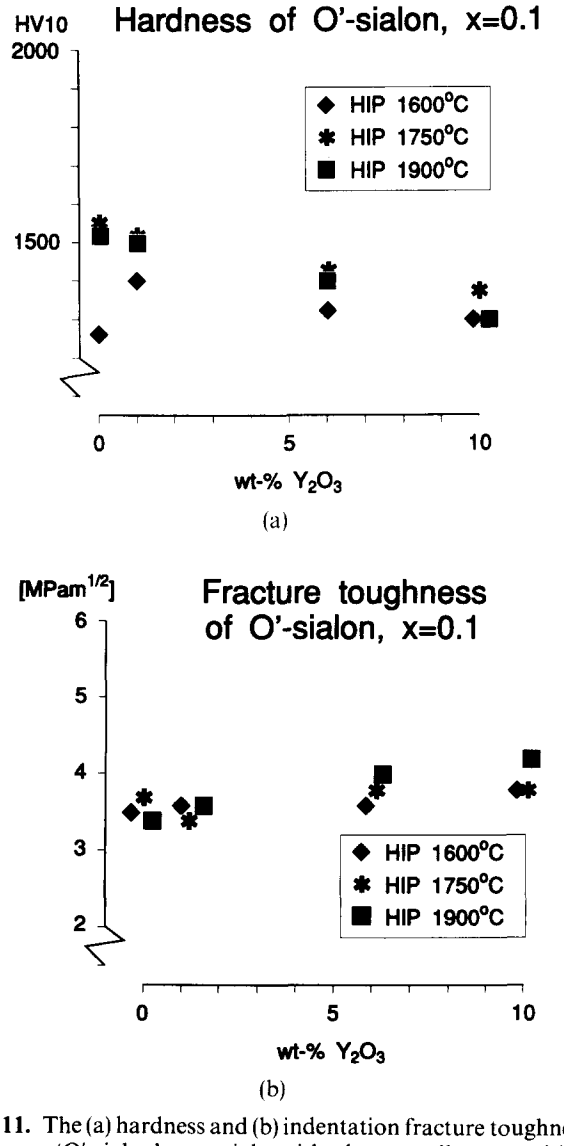

Fig. 11. The (a) hardness and (b) indentation fracture toughness of dense 'O'-sialon' materials with the overall composition $x = 0·1$, prepared by HIP and with different amounts of yttria added. Note that the specimen with no yttria added HIPed at 1600°C contains no O'-sialon phase, whereas the yields for the other samples are above 80%, cf. Table 1.

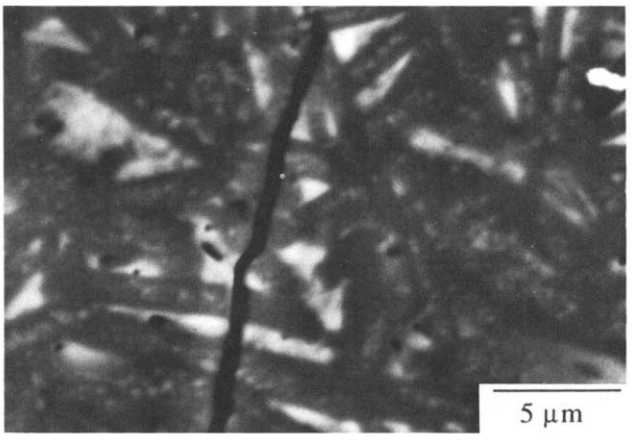

Fig. 12. Crack originating from a Vickers indentation mark in the sample with $x = 0·1$ containing 6 wt% Y_2O_3 HIPed at 1900 C.

different temperatures thus converged somewhat within increasing amount of Y_2O_3 dopant; this can be exemplified by the hardness of materials containing 10 wt% Y_2O_3, all falling within the range 1250–1400 despite the differences in preparation temperature.[11]

Additions of alumina ($x = 0·1$) resulted in an increase in hardness for the series sintered at 1750°C to about 1550, but did not significantly change the hardness of the materials sintered at the other two temperatures without yttria addition (see Fig. 11). Simultaneous yttria additions to samples having $x = 0·1$ resulted in a slight increase in fracture toughness, from about 3·5 to 4 MPa $m^{1/2}$, and a slight decrease in hardness to 1300–1400, cf. Fig. 11. The cracks originating from the Vickers indentations were found to proceed through the grains (see Fig. 12), rather surprisingly, since the occurrence of elongated crystals normally forces cracks to deviate.

4 Discussion

It was observed that alumina or yttria additions and higher temperatures enhance the formation of Si_2N_2O. This is in accordance with several previous publications, where it has been shown that the presence of a liquid phase at the sintering temperature is needed to overcome sluggish sintering kinetics and to facilitate the oxynitride formation.[7–11] Thus, it seems that the sintering temperature must exceed a minimum value for the silicon oxynitride formation. Bergman and Heping[10] used Al_2O_3, MgO or Y_2O_3 as dopants and noticed that no Si_2N_2O was formed at temperatures below 1500–1550°C. The maximum formation of Si_2N_2O with these dopants was found to be 55% (Al), 80% (Mg) and 80% (Y) at 1700°, 1600° and 1600°C, respectively. Bergman and Heping[10] also observed a strongly increasing weight loss from the samples at

temperatures above 1600°C and concluded that this temperature therefore was the highest of practical interest. Lewis *et al.*[12] prepared dense O′-sialon ceramics at about 1650°C by PS and simultaneous additions of Al_2O_3 and Y_2O_3. Trigg and Jack[14] showed similar densification results by PS and found no O′-sialon formation at 1500°C, but at 1600°, 1700° and 1800°C the yields of O′-sialon were about 70%, 90% and 100%, respectively. However, the latter authors also noticed a decrease in the densities of O′-sialon ceramics prepared by PS at temperatures above 1600°C, due to the volatilization of silicon monoxide and nitrogen with consequent bloating. Thus it seems that about 1600–1650°C should be the highest possible temperature to use for pressureless sintering without a decrease in density.

The previously reported results in the literature are in accordance with the findings in this study, where pressureless sintering at high temperatures was found to be unfavourable, as a decomposition process with gas evolution caused porosity in the materials. The decomposition and formation of porosity by trapped gas was found to be greatly reduced by HIP, even at high temperatures. Increasing the temperature, however, had another negative effect. The amount of intergranular phase was found to increase greatly at high temperatures, probably as a consequence of the fact that the liquid phase region in the Y–Si–O–N or Y–Si–Al–O–N systems increases rapidly with temperature. Thus, it is possible that the relative amount of Si_2N_2O or O′-sialon decreases at high temperatures, even if the analysis by X-ray diffraction at a first glance seems to yield a higher 'Si_2N_2O' content by temperature. Another effect complicating the phase composition of the sample is the possibility that upon cooling from the high sintering temperature, some 'Si_2N_2O' might rapidly reprecipitate from the supersaturated liquid. Crystals of Si_2N_2O were found in the electron microscopy analysis in the form of very fine particles distributed in the intergranular residual glassy phase at room temperature. Therefore, even if X-ray diffraction analysis of high temperature sintered materials indicates high 'Si_2N_2O' yields, the microstructures might be very complex multiphase aggregates.

A common feature of the different samples investigated in this work is the occurrence of bright rounded areas inside the O′-sialon grains, corresponding to 'Si_3N_4'-crystals. The fact that these crystals are found inside the O′-sialon grains indicates that these two phases are both present from the start or form early during the sintering process. The round shape of the 'Si_3N_4' inclusions indicates that these crystals had been partly dissolved by the liquid at the time of encapsulation into the Si_2N_2O crystals. Possibly, some of the 'Si_3N_4' crystals might have functioned as crystallization seeds for the formation of the large O′-sialon grains. These inclusions of 'β-Si_3N_4' strongly affect the O′-sialon grains, causing a large amount of defects in the crystal. As discussed below, one contribution to the low fracture toughness observed might arise from these inclusions and defects in the Si_2N_2O type crystals, which possibly also may reduce the strength of the material.

No evidence was found, either by EDS/WDS analysis of the grains or by XRD analysis of the lattice parameters, that yttrium enters the Si_2N_2O phase in materials sintered with Y_2O_3 added. The intergranular glassy phase contained all the added yttrium. This result is different to what has been reported by Sjöberg *et al.*[17] who found that some yttrium, below 1·5 wt%, may enter the O′-sialon structure. One explanation of this discrepancy might be inclusions of Y-rich phases, similar to the Si_3N_4 inclusions frequently observed in this study. It has recently been found by careful EDX/STEM analysis of the Si_2N_2O grains in hot-pressed Si_3N_4–ZrO_2(+Y_2O_3) composites that inclusions of both β-Si_3N_4 and an Y-containing phase were present.[18] However, in the latter study no detectable amounts of Y were found dissolved in the Si_2N_2O structure, besides the Y-rich inclusions, in accordance with our results.

When no yttria was added, increasing amount of alumina added resulted in an increasing amount of Al being substituted into the Si_2N_2O structure, as clearly demonstrated by the shift in the unit cell parameters. However, when yttria was added together with alumina, a considerable amount of glassy intergranular phase was formed consisting of a Y–Al–silicate glass, removing Al from the O′-sialon phase in the process. This behaviour would be expected from the large extension of the glassy area into the Y–Si–Al–O–N phase diagram.[19] As a consequence, the added aluminium will be distributed in the O′-sialon phase, the glassy phase and, to some small extent, also in the Si_3N_4 structure (β-sialon).

The EDS analysis in TEM showed that the yttrium content in the Y–Si–Al–O–N glassy phase varied on a micro-scale from one glassy pocket to another. This observation is in accordance with previous reports on Si_2N_2O ceramics doped with 6 wt% Al_2O_3 and 10 wt% Y_2O_3. For these materials, a compositional variation was noted, and a separation of the amorphous material into two glassy phases was also observed.[17] Both glassy phases contained Y, Si and Al, but the dominating continuous glassy region was richer in Y and contained some rounded inclusions of an Si-rich glass.

The difference in the formation of O′-sialon by

pressureless sintering and HIP at 1600°C is somewhat surprising. The reason is not clearly understood, but the temperature is close to the expected eutectic for the oxynitride melt, which makes the sintering process very temperature-sensitive. Thus a small change in temperature from the nominal value might radically change the amounts of the different phases formed during the sintering process.

The fracture toughness of the Si_2N_2O oxynitride ceramics was generally low, about 3·5 MPa $m^{1/2}$, and did not improve significantly with the addition of yttria. Additions of alumina alone or simultaneous additions of alumina and yttria increased the toughness slightly to about 4 MPa $m^{1/2}$, but the materials obtained must still be regarded as very brittle. With low amounts of dopants and high sintering temperatures (high 'Si_2N_2O' contents) the material was fairly hard, *HV10* about 1500, which can be compared to low-doped Si_3N_4 ceramics with *HV10* around 1700. However, increasing amounts of sintering aids caused by hardness of the Si_2N_2O ceramics to fall, probably as a consequence of the increasing amount of glassy grain-boundary phase (*HV* about 800–1000).

The poor toughness behaviour of the yttria-doped silicon oxynitride ceramics, despite the formation of elongated plate-like grains, might be due to the high defect concentration in the crystals making them brittle or to the bonding being 'too strong' between the Si_2N_2O crystals and the glassy phase. In both cases the crack should proceed straight through both the glass and the crystals and thus no pull-out, crack-deflection or crack-branching effects will contribute to the fracture toughness. Similar low toughness levels, as well as a fairly low strength of fully dense Si_2N_2O ceramics prepared by HIP, were noted by Larker.[6] The effects of the crystal-to-glassy phase bond was shown by Ohashi[5,8] who reported that a ceria-doped Si_2N_2O material with a glassy grain-boundary phase had a fracture toughness of 2·5 (MPa $m^{1/2}$). Heat treatment of the same material, in order to crystallize the glassy phase, had a dramatic effect on the toughness, increasing it to about 5·5. In the heat-treated material, the bonding between the crystallized intergranular phase and the Si_2N_2O crystals was much weaker.

5 Conclusions

Densification of Si_2N_2O materials by pressureless sintering with only Y_2O_3 added was promoted by high temperatures, but fully dense materials were not achieved (98–99% TD). Addition of Al_2O_3 only, to form O'-sialon, greatly enhanced the densification and gave fully dense materials at 1600°C, as did also simultaneous addition of Y_2O_3 and Al_2O_3 at this low temperature. Increasing the temperature in pressureless sintering to 1775°C caused porosity to occur in all materials.

Samples of the HIPed materials, containing additions of Y_2O_3, needed temperatures of 1750°C or higher to form Si_2N_2O in significant amounts. However, the addition of Al_2O_3 enhanced the formation of O'-sialon even at 1600°C.

The lattice parameters of the orthorhombic unit cell of O'-sialon and the cell volume increased with increasing x-value in $Si_{2-x}Al_xO_{1+x}N_{2-x}$. Refinement of the lattice parameters of the O'-sialon phase was a good indicator of the overall Al content and it was demonstrated from the shifts in the lattice parameters that even small additions of yttria extracted Al from the O'-sialon crystals into a glassy intergranular phase.

The crystals of Si_2N_2O or O'-sialon formed had high aspect ratios, typically 7–10. In all materials some glassy intergranular phase and β-Si_3N_4 crystals were present, i.e. monophasic materials were never prepared. Part of the β-Si_3N_4 was found as inclusions in the Si_2N_2O structure, causing a very high lattice defect population.

Dense O'-sialon materials were hard (*HV10* about 1500) and fairly brittle (K_{1C} about 3·5 MPa $m^{1/2}$) at room temperature. The hardness decreased slightly and the fracture toughness increased to about 4 MPa $m^{1/2}$ with increasing alumina and yttria content.

Despite the presence of grains with an elongated plate-like form of high aspect ratio, the materials were brittle. One reason for this might be the high defect concentration in the large Si_2N_2O or O'-sialon grains. Another cause might be a too strong interfacial bond between crystal and glass to allow toughening effects.

References

1. Heuer, A. H. & Lou, V. L. K., Volatility diagrams for silica, silicon nitride and silicon carbide, and their application to high-temperature decomposition and oxidation. *J. Am. Ceram. Soc.*, **73** (1990) 2785–803.
2. Billy, M. & Desmaison, J. G., High temperature oxidation of silicon-based structural ceramics. *High Temp. Technol.*, **4** (1986) 131–9.
3. O'Meara, C., Sjöberg, J., Dunlop, G. & Pompe, R., Oxidation of pressureless sintered Si_2N_2O materials. *J. Europ. Ceram. Soc.*, **7** (1991) 369–78.
4. Persson, J., Käll, P. O., Nygren, M. & Larker, R., Oxidation studies of Si_2N_2O. In *Proc. 4th Intern. Symp. Ceram. Mater. Eng.*, ed. R. Carlsson, T. Johansson & L. Kahlman. Elsevier Applied Science Publishers, 1992, pp. 1187–94.
5. Ohashi, M., Kanzaki, S. & Tabata, H., Processing, mechanical properties and oxidation behaviour of silicon oxynitride ceramics. *J. Am. Ceram. Soc.*, **74** (1991) 109–14.
6. Larker, R., Reaction sintering and properties of silicon oxynitride densified by HIP. *J. Am. Ceram. Soc.*, **75** (1992) 62–6.

7. Huang, Z. K., Greil, P. & Petzow, G., Formation of silicon oxynitride from Si_3N_4 and SiO_2 in the presence of Al_2O_3. *Ceram. Int.*, **1** (1984) 14–17.
8. Ohashi, M., Kanzaki, S. & Tabata, H., Effect of additives on some properties of silicon oxynitride ceramics. *J. Mater. Sci.*, **26** (1991) 2608–14.
9. Barta, J., Manela, M. & Fischer, R., Si_3N_4 and Si_2N_2O for high performance radomes. *Mater. Sci. Eng.*, **71** (1985) 265–72.
10. Bergman, B. & Heping, H., The influence of different oxides on the formation of Si_2N_2O from SiO_2 and Si_3N_4. *J. Europ. Ceram. Soc.*, **6** (1990) 3–8.
11. Ekström, T., Holmstöm, M. & Olsson, P. O., Yttria doped Si_2N_2O ceramics. In *Proc. 4th Intern. Symp. Ceram. Mater. Eng.*, ed. R. Carlsson, T. Johansson & L. Kahlman. Elsevier Applied Science Publishers, 1992, pp. 432–9.
12. Lewis, M. H., Reed, C. J. & Butler, N. D., Pressureless-sintered ceramics based on the compound Si_2N_2O. *Mater. Sci. Eng.*, **71** (1985) 87–94.
13. Trigg, M. B. & Jack, K. H., Solubility of aluminium in silicon oxynitride. *J. Mater. Sci. Letters*, **6** (1987) 407–8.
14. Trigg, M. B. & Jack, K. H., The fabrication of O′-sialon ceramics by pressureless sintering. *J. Mater. Sci.*, **23** (1988) 481–7.
15. Ekström, T., Käll, P.-O., Nygren, M. & Olsson, P.-O., Dense single-phase beta-sialon ceramics by glass-encapsulated hot isostatic pressing. *J. Mater. Sci.*, **24** (1989) 1853–61.
16. Olsson, P.-O., Crystal defects and coherent intergrowth of α- and β-crystals in Y-Ce doped sialon materials. *J. Mater. Sci.*, **24** (1989) 3878–87.
17. Sjöberg, J., O'Meara, C. & Pompe, R., The effect of yttria additions on the composition of O′-sialons prepared by pressureless sintering. *J. Europ. Ceram. Soc.*, **10** (1992) 41–50.
18. Falk, L. K. L. & Rundgren, K., Microstructure and short-term oxidation of hot-pressed $Si_3N_4/ZrO_2(+Y_2O_3)$ ceramics. *J. Am. Ceram. Soc.*, **75** (1992) 28–35.
19. Thompson, D. P., Phase relationships in Y–Si–Al–O–N ceramics. *Mater. Sci. Research*, **20** (1988) 79–91.